Finite-element analysis of beams and plates with moving loads

Autor(en):   **Yoshida, David M. / Weaver, William Jr.**

Finite-Element Analysis of Beams and Plates with Moving Loads

Analyse des éléments finis pour poutres et plaques sous l'influence de charges mobiles

Analyse der endlichen Elemente für Träger und Platten bei bewegter Last

DAVID M. YOSHIDA
Director, Accident Analysis Associates,
Palo Alto, California

WILLIAM WEAVER, JR.
Professor of Structural Engineering,
Stanford University, Stanford, Calif.

Introduction

The first investigators of the problem of moving loads on structures were primarily concerned with the response of railway bridges as heavy locomotives passed over. When engineers of today design lightweight highway bridges, the dynamic response of these structures due to the passage of semi-trucks and other large vehicles becomes important. In addition, rapid-transit systems introduce problems involving elevated structures subjected to loads traveling at high speeds. An analysis technique for predicting the dynamic response of such structures to moving loads is essential to a reliable design.

The problem of a massless beam traversed by a single unsprung mass was first considered by WILLIS [19, 20] and later solved by STOKES [14], who also showed a solution for a beam of uniform mass with a force moving at constant velocity. Variations of these original problems have subsequently been studied by many other investigators, including TIMOSHENKO, who contributed a solution for the case when the magnitude of the force varies hormonically [15].

JEFFCOTT [10] studied the effect of an unsprung mass moving with constant velocity over a simply-supported beam. Later INGLIS [9], LOONEY [12], and HILLERBORG [7] introduced to Jeffcott's problem the simplifying assumption that the deflected shape of the beam due to the moving load at any time is proportional to the first natural mode of the unloaded beam. TUNG, et al., [16] and BIGGS, et al., [2] also have used this assumption in their analyses. The latter group compared their work with laboratory and field test results and found acceptable correlation for low highway speeds. Another simplifying assumption, that the deflected shape of the beam at any time is proportional

to its instantaneous static deflection curve, was used by HILLERBORG [8] and
WEN [18].

FLEMING and ROMUALDI [6] studied single- and multiple-span beams
using an average-velocity method to solve the differential equations. They
considered many effects, such as the masses of the load and the beam, springing
of the load, damping of both load and beam, and variable beam cross sections.
VELETSOS and HUANG [17] have reported upon comprehensive studies of multi-
axle trucks moving across highway bridges idealized as continuous beams
with lumped masses and absolute damping. In their project, the equations of
motion were integrated step-by-step, using the linear-acceleration method.

The dynamic response of both beams and frames to constant-velocity
moving forces was investigated by FILHO [5] using lumped-mass analytical
models for the structures. Furthermore, WILSON and TSIRK [22] introduced
a framework analogy to model a plate traversed by constant-velocity moving
loads. However, the use of discrete-parameter systems for the analysis of
beams and plates under moving loads has not been fully developed.

In this paper the method of finite elements is used to model continuous
beams and rectangular plates traversed by moving loads. Equations of motion
for discretized beams and plates are solved for constant-velocity and constant-
acceleration cases of moving loads with and without the influence of a mass
associated with the load itself. When only the force is considered, the analysis
is linear and will be referred to as the moving-force problem. When the effect
of the mass is also to be considered, the analysis is nonlinear; and it will be
called the moving-mass problem.

Computer programs for the linear and nonlinear analyses of beams and
plates yield plotted results for selected illustrative examples. Response curves
are compared with the results of other investigators wherever possible, but
the methods utilized in this study are capable of producing results for problems
not previously solved.

Analytical Models

Several finite-element models have been developed to represent prismatic
beams and rectangular plates. The models vary in complexity; and some
yield exact results, depending upon the nature of the problem. Since the
finite-element method is well documented [13], only brief summaries for the
elements utilized in this study are given herein. Both the beam and the plate
elements are based upon assumed shape functions.

Beam Element

Fig. 1a shows the prismatic beam element (of length l) used in this study,
and Fig. 1b depicts the static shape function for nodal displacement $D_1 = 1$.
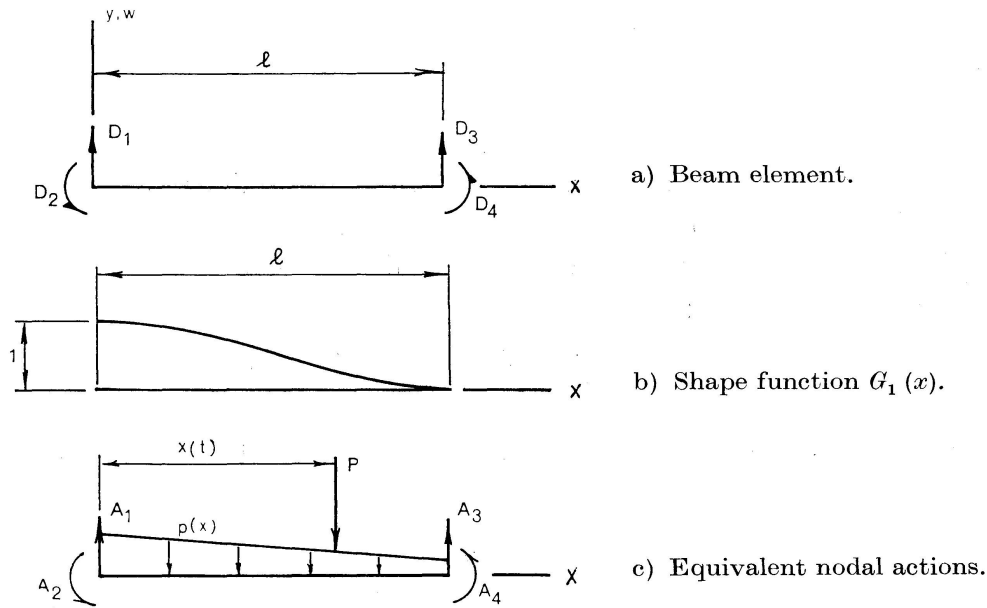
Fig. 1.

Shape functions assumed for the four types of nodal displacements of this element are:

$$G_1(x) = 1 - \frac{3x^2}{l^2} + \frac{2x^3}{l^3}, \qquad G_2(x) = x - \frac{2x^2}{l} + \frac{x^3}{l^2},$$

$$G_3(x) = \frac{3x^2}{l^2} - \frac{2x^3}{l^3}, \qquad G_4(x) = -\frac{x^2}{l} + \frac{x^3}{l^2}. \tag{1}$$

The generic displacement $w(x)$ of the beam element can be expressed in terms of the shape functions $\underset{\sim}{G}(x)$ and the nodal displacements $\underset{\sim}{D}$ by use of the principle of superposition, which results in:

$$w(x) = \underset{\sim}{G}^T(x)\,\underset{\sim}{D} = [G_1(x),\, G_2(x),\, G_3(x),\, G_4(x)] \begin{Bmatrix} D_1 \\ D_2 \\ D_3 \\ D_4 \end{Bmatrix}. \tag{2}$$

It should be noted that the generic displacement is a cubic polynomial in x; therefore, it can represent displacement states for concentrated loads exactly.

The element stiffness matrix for the beam, in terms of the second derivatives of the beam shape functions, is given by:

$$\underset{\sim}{S} = EI \int_0^l \underset{\sim}{G}_{xx}(x)\, \underset{\sim}{G}_{xx}^T(x)\, dx, \tag{3}$$

in which E is Young's modulus and I is the moment of inertia.

Energy-equivalent nodal actions for a beam element appear in Fig. 1 c. For a distributed loading they are:

$$\underset{\sim}{A} = \int_0^l p(x)\, \underset{\sim}{G}(x)\, dx. \tag{4}$$

However, for the particular case of the moving load P shown in the figure, Eq. (4) becomes:

$$\underset{\sim}{A}(t) = P\,\underset{\sim}{G}\,[x(t)].\tag{5}$$

In this case the position of the load and the equivalent nodal actions are functions of time, and no integration is required.

The energy-consistent mass matrix of the beam element has been shown by Archer [1] to be:

$$\underset{\sim}{M} = \mu\,A\int_0^l \underset{\sim}{G}(x)\,\underset{\sim}{G}^T(x)\,dx,\tag{6}$$

in which μ is the mass density of the beam and A denotes its cross-sectional area.

Plate Element

The plate-bending element applied in this study is shown in Fig. 2 along with the nodal displacements and a local coordinate system. Compatible shape
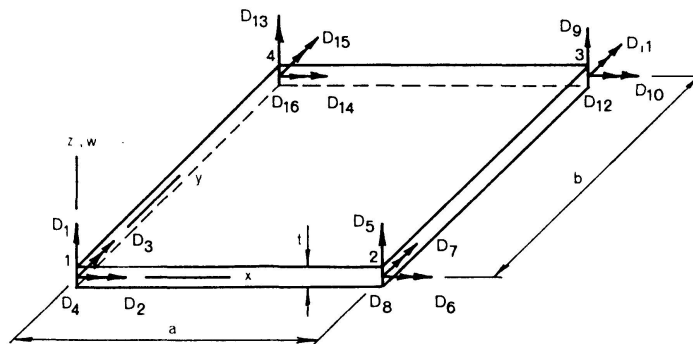
Fig. 2. Plate element.

functions for the rectangular plate element were first derived by Bogner et al., [3]. They are closely related to the beam shape functions and can be represented by products of such functions as follows:

$$
\begin{aligned}
G_1\,(x,y) &= f_1(x)f_1(y), & G_2\,(x,y) &= f_1(x)g_1(y),\\
G_3\,(x,y) &= -g_1(x)f_1(y), & G_4\,(x,y) &= -g_1(x)g_1(y),\\
G_5\,(x,y) &= f_2(x)f_1(y), & G_6\,(x,y) &= f_2(x)g_1(y),\\
G_7\,(x,y) &= -g_2(x)f_1(y), & G_8\,(x,y) &= -g_2(x)g_1(y),\\
G_9\,(x,y) &= f_2(x)f_2(y), & G_{10}\,(x,y) &= f_2(x)g_2(y),\\
G_{11}\,(x,y) &= -g_2(x)f_2(y), & G_{12}\,(x,y) &= -g_2(x)g_2(y),\\
G_{13}\,(x,y) &= f_1(x)f_2(y), & G_{14}\,(x,y) &= f_1(x)g_2(y),\\
G_{15}\,(x,y) &= -g_1(x)f_2(y), & G_{16}\,(x,y) &= -g_1(x)g_2(y).
\end{aligned}\tag{7}
$$

The first terms in the product functions in Eqs. (7) are the beam shape functions shown in Eqs. (1) related by: $f_1(x) = G_1(x)$, $f_2(x) = G_3(x)$, $g_1(x) = G_2(x)$,

and $g_2(x) = G_4(x)$, in which the length l is replaced by a, the x-dimension of the plate. The second terms in the product functions are obtained from the beam shape functions in a similar manner, using b in place of l. The minus sign appearing in half of the expressions is due to the difference in the sign conventions for the slope term w_x and the associated nodal displacements D_3, D_7, D_{11}, and D_{15}. Furthermore, the twist curvature w_{xy} and its associated nodal displacements D_4, D_8, D_{12}, and D_{16} also differ in sign. The generic displacement $w(x,y)$ of the plate element in terms of these displacement functions is:

$$w(x,y) = \underset{\sim}{G}^T(x,y)\,\underset{\sim}{D}. \tag{8}$$

The stiffness matrix for the plate-bending element involves second partial derivatives of the shape functions as follows:

$$\underset{\sim}{S} = R\int_0^b\int_0^a[\underset{\sim}{G}_{xx}\,\underset{\sim}{G}_{xx}^T + \underset{\sim}{G}_{yy}\,\underset{\sim}{G}_{yy}^T + 2\,\nu\,\underset{\sim}{G}_{xx}\underset{\sim}{G}_{yy}^T + 2\,(1-\nu)\,\underset{\sim}{G}_{xy}\underset{\sim}{G}_{xy}^T]\,dx\,dy, \tag{9}$$

where ν is Poisson's ratio, and the plate rigidity R is

$$R = \frac{E\,t^3}{12\,(1-\nu^2)} \tag{10}$$

and t is the plate thickness.

Analogous to Eq. (6), the consistent-mass matrix for the plate element may be deduced to be:

$$\underset{\sim}{M} = \mu\,t\int_0^b\int_0^a\underset{\sim}{G}(x,y)\,\underset{\sim}{G}^T(x,y)\,dx\,dy. \tag{11}$$

The equivalent nodal actions due to concentrated moving loads require no integrations.

$$\underset{\sim}{A}(t) = P\,\underset{\sim}{G}[x(t),y(t)]. \tag{12}$$

If the force is restricted to move along the element interface, where $y = 0$ or $y = b$, then only four shape functions are involved; and the equivalent nodal actions become the same as those for the beam element. Furthermore, the position of the load $x(t)$ as it traverses a beam or plate element will be restricted to the case of constant acceleration, as expressed by:

$$x(t) = v_0\,t + \tfrac{1}{2}a_0\,t^2, \tag{13}$$

where v_0 represents a positive entrance velocity at the left side of the element and a_0 is the value of constant acceleration of the load. It can be seen from Eq. (5) that the equivalent nodal actions of a force whose position is given by Eq. (13) become explicit functions of time. Furthermore, these actions are at most sixth degree polynomials in time, because the shape functions are cubic in x (which is in turn quadratic in time).

Moving-Force Problems

The moving-force problem results in a finite number of linear differential equations of motion for the nodes of the structure, which are solved by the normal-mode method. Because the energy-consistent stiffness and mass matrices are identically banded, the generalized LANCZOS method [11, 23] serves the useful purpose of diagonalizing the stiffness matrix and reducing the mass matrix to tridiagonal form. Then the eigenvalues and eigenvectors of the system are evaluated by the Q-R algorithm, and the remainder of the normal-mode analysis follows the pattern explained below.

Solution by Normal Modes

For either the beam or the plate problem the equations of motion for the discretized system without damping can be stated as:

$$M \ddot{D} + S D = A (t),   (14)$$

where D and $\ddot{D}$ are nodal displacements and accelerations, respectively, M and S are the consistent-mass and stiffness matrices, and $A (t)$ represents equivalent nodal actions due to the moving force. Transformation to normal coordinates produces a set of n uncoupled equations, which may be represented by the expression:

$$\ddot{x}_i + p_i^2 x_i = p_i^2 \sum_{k=1}^{n} r_{ki} A_k (t),   (15)$$

in which x_i is the i-th normal coordinate, p_i is the i-th circular frequency, and r_{ki} represents the k-th nodal displacement in the i-th normal mode.

The general solution of Eq. (15) in terms of Duhamel's integral is given by:

$$x_i (t) = x_{i0} \cos p_i t + \frac{\dot{x}_{i0}}{p_i} \sin p_i t + p_i \sum_{k=1}^{n} r_{ki} \int_0^t A_k (\tau) \sin p_i (t - \tau) d\tau,   (16)$$

where x_{i0} and $\dot{x}_{i0}$ are the initial displacement and velocity of the i-th normal coordinate. If the structural system starts from rest, the initial conditions (x_{i0} and $\dot{x}_{i0}$) are zero before the first element is traversed by a moving load.

When the moving force reaches the end of an element and starts across the next, two changes occur: First, the shape functions of the next element are used to compute the equivalent nodal actions, which are nonzero while the load traverses the element. Second, the initial conditions associated with the next element must be computed from the final values of the previous element. These initial conditions need be computed only in normal coordinates from Eq. (16) and its first time derivative.

Transformation of the solution back to nodal coordinates gives the dynamic displacement of the j-th degree of freedom as:

$$D_j = \sum_{i=1}^{n} r_{ji} \left(x_{i\,0} \cos p_i t + \frac{\dot{x}_{i\,0}}{p_i} \sin p_i t \right) + \sum_{i=1}^{n} \sum_{k=1}^{n} p_i r_{ji} r_{ki} \int_0^t A_k(\tau) \sin p_i(t-\tau) d\tau. \quad (17)$$

Because of the specific shape functions and the type of motion assumed, it is necessary to evaluate Duhamel integrals for each nonzero nodal action of the following form:

$$\int_0^t A_k(\tau) \sin p_i(t-\tau) d\tau = \int_0^t (\alpha_0 + \alpha_1 \tau + \cdots + \alpha_6 \tau^6) \sin p_i(t-\tau) d\tau, \quad (18)$$

where the constants $\alpha_0, \alpha_1, \ldots, \alpha_6$ are determined from Eqs. (1), (5), and (13). For example, the nodal action A_1 for the beam element expressed as a function of time is:

$$A_1 = P \left[1 - \frac{3}{l^2} \left(v_0 t + \frac{1}{2} a_0 t^2 \right)^2 + \frac{2}{l^3} \left(v_0 t + \frac{1}{2} a_0 t^2 \right)^3 \right]. \quad (19)$$

Therefore, the constants in Eq. (18) for this case become:

$$\alpha_0 = 1, \qquad \alpha_1 = 0, \qquad \alpha_2 = -\frac{3 v_0^2}{l^2}, \qquad \alpha_3 = -\frac{3 v_0 a_0}{l^2} + \frac{2 v_0^3}{l^3},$$

$$\alpha_4 = -\frac{3}{4} \frac{a_0^2}{l^2} + \frac{3 v_0^2 a_0}{l^3}, \qquad \alpha_5 = \frac{3}{2} \frac{v_0 a_0^2}{l^3}, \qquad \alpha_6 = \frac{1}{4} \frac{a_0^3}{l^3}. \quad (20)$$

The constants for the other nodal actions may be obtained in a similar manner, and the evaluation of the Duhamel integrals is accomplished through repeated integrations by parts.

Beam Example

Fig. 3 shows a simply-supported beam modeled by four finite elements.
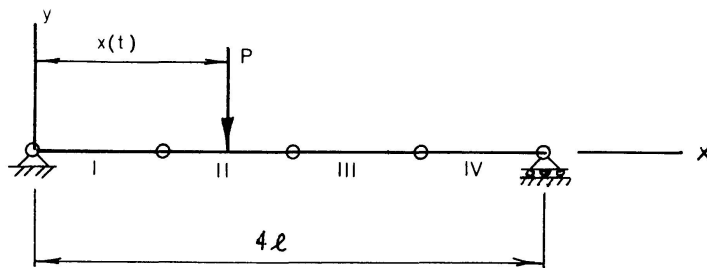
Fig. 3. Beam example.

This example will serve to demonstrate the method and to compare solutions with known results. Dynamic response of the center of the beam is obtained for both constant-velocity and constant-acceleration moving forces. The magnitude of the traveling force is one pound for all beam solutions. Physical properties of the beam (having cross-sectional dimensions $= \frac{1}{4}$ in. $\times \frac{1}{4}$ in.) are taken as:

$$E = 30 \cdot 10^6 \,\text{psi}, \qquad \mu = 0.001 \,\text{lb-sec}^2/\text{in.}^4,$$

$$A = 0.0625 \,\text{in.}^2, \qquad I = 3.255 \cdot 10^{-4} \,\text{in.}^4, \quad l = 1 \,\text{in.},$$

$$\text{Fundamental Period:} \quad T_1 = 8.149 \cdot 10^{-4} \,\text{sec}.$$

For the constant-velocity case it has been shown (4) that the maximum dynamic displacement occurs when the travel time T (the time required for the force to traverse the span) is near the fundamental period ($T = 0.82\,T_1$). Therefore, travel times were chosen in proportion to the fundamental period. For the constant-acceleration case it is assumed that the force starts with zero velocity and accelerates across the span in such a manner that the desired travel time is attained.

Table 1 contains results for five different travel times, and Fig. 4 shows computer plots of the solutions for the cases of travel time equal to the fundamental period. The ordinate in Fig. 4 represents the center displacement divided by the static maximum, and the abscissa is real time divided by the travel time. The constant-velocity curve is identified by w_v, the constant-acceleration curve by w_a, and the static influence curve is shown without a label.

Fig. 4. Beam response to moving force.

Table 1. Dynamic Magnification Factors for Moving Force on Beam

$\dfrac{T_1}{T}$	v_0 (inches/second)	$\dfrac{w_v}{w_{st}}$	$\dfrac{w_v}{w_{st}}$ (Filho)	$\dfrac{w_v}{w_{st}}$ (Exact)	a_0 (inches/second^2) $\times 10^5$	$\dfrac{w_a}{w_{st}}$
(1)	(2)	(3)	(4)	(5)	(6)	(7)
$\frac{1}{8}$	614	1.055	—	1.045	1.882	1.005
$\frac{1}{4}$	1228	1.112	1.11	1.108	7.530	1.032
$\frac{1}{2}$	2456	1.251	1.24	1.250	30.12	1.091
1	4912	1.700	1.68	1.707	120.5	1.525
2	9824	1.540	1.54	1.550	481.9	1.310

Dynamic magnification factors for both the constant-velocity and the constant-acceleration cases were computed by dividing the maximum dynamic displacement of each by the static maximum. These factors are listed in columns 3 and 7 of Table 1, while columns 2 and 6 give the velocities and accelerations for those cases. Column 4 in the table contains results obtained by FILHO [5] for a constant-velocity moving force, using a discrete model with lumped masses. An exact solution is also available (4) for this case and is included in column 5. It is apparent from the tabulated results that the finite-element model with the consistent-mass representation closely approximates the known solution of the constant-velocity case.

Plate Example

To demonstrate the potential of the plate model, we consider the square plate simply-supported on all sides, as shown in Fig. 5. The dynamic response
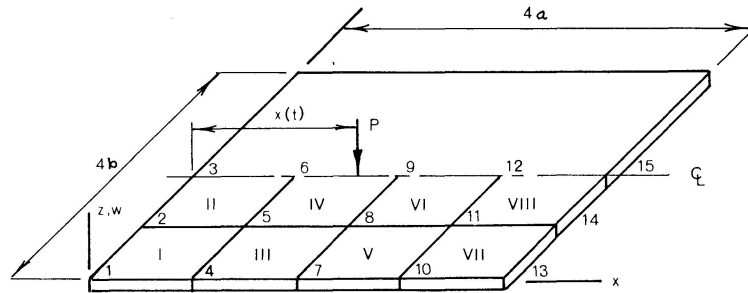
Fig. 5. Plate example.

of the plate is obtained for a moving force that travels along the centerline drawn on the figure. Physical properties of the plate are as follows:

$$E = 30 \cdot 10^6 \text{ psi}, \qquad t = 0.1 \text{ in.}, \quad \nu = 0.3,$$
$$\mu = 0.001 \text{ lb-sec}^2/\text{in.}^4, \quad a = b = 1 \text{ in.},$$
$$\text{Fundamental Period:} \quad T_1 = 9.7172 \cdot 10^{-4} \text{ sec},$$

Because this system has symmetry about one axis, only half of the plate need be modeled (using eight elements), as shown in Fig. 5. The magnitude of the moving force is two pounds for all cases studied; thus, the force on half the plate is one pound.

The same ratios between the fundamental period T_1 and travel time T used for the beam were used again for the plate, and solutions were obtained for the dynamic response at the midpoint. Fig. 6 shows plots of the solutions for constant-velocity and constant-acceleration moving forces with $T = T_1$. Dynamic magnification factors computed for each case are presented in Table 2. Included as column 4 of this table are constant-velocity results obtained by WILSON and TSIRK [22], using a framework analogy with a lumped-mass representation. Exact analyses for moving forces on plates are not available.
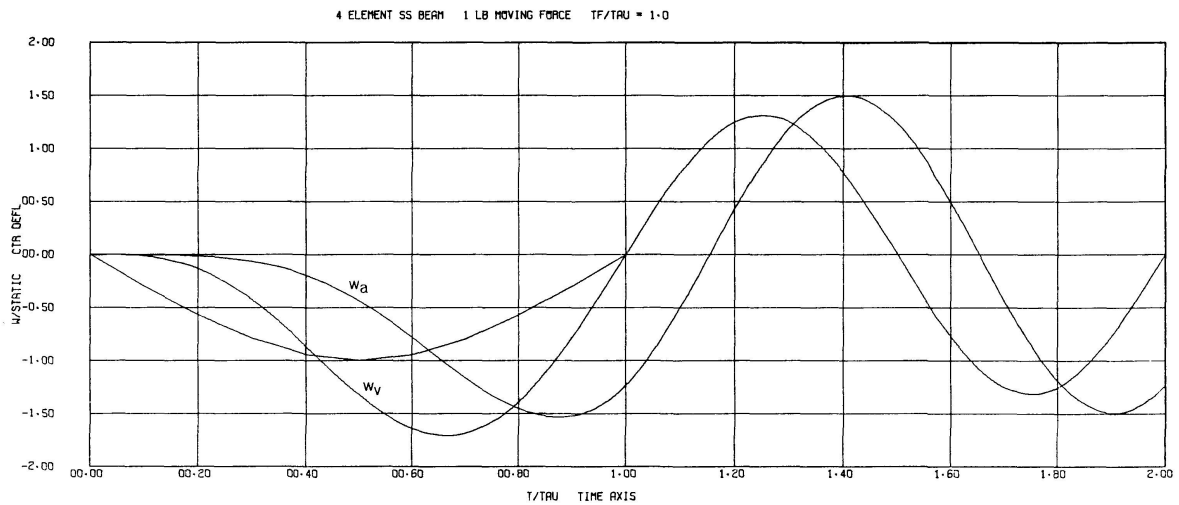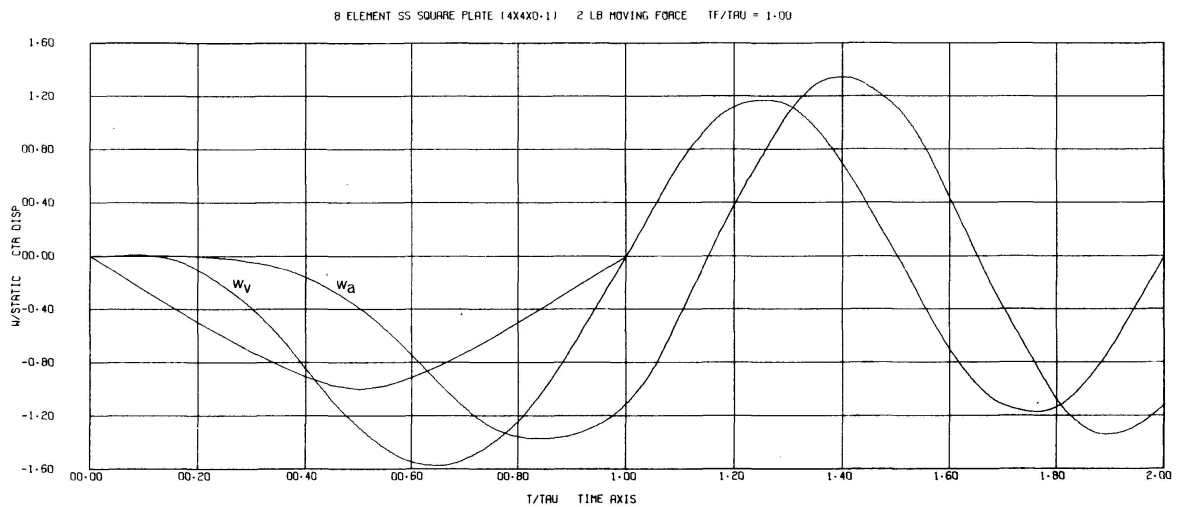
Fig. 6. Plate response to moving force.

Table 2. Dynamic Magnification Factors for Moving Force on Plate

$\dfrac{T_1}{T}$	v_0 (inches/ second)	$\dfrac{w_v}{w_{st}}$	$\dfrac{w_v^+}{w_{st}}$	a_0 (inches/ second²) $\times 10^5$	$\dfrac{w_a}{w_{st}}$
(1)	(2)	(3)	(4)	(5)	(6)
$\frac{1}{8}$	515	1.042	—	1.324	0.990
$\frac{1}{4}$	1030	1.088	1.111	5.295	1.020
$\frac{1}{2}$	2060	1.200	1.216	21.18	1.071
1	4120	1.568	1.510	84.72	1.370
2	8240	1.390	—	338.9	1.265

Moving-Mass Problems

The moving-mass problem produces a finite number of nonlinear differential equations, the coefficients of which depend upon the speed of the moving load. Solutions for this class of problem are obtained by the linear acceleration method of numerical integration. For this purpose the equations are cast into a special form suitable for step-by-step analysis.

Formulation

The moving mass is assumed not to lose contact with the structure as it traverses the span. Therefore, its displacement, velocity, and acceleration must be the same as that of the point of contact, as follows:

$$w(x,t) = w[x(t),t], \tag{21}$$

$$\dot{w}(x,t) = \frac{\partial w}{\partial x}\dot{x} + \frac{\partial w}{\partial t}, \tag{22}$$

$$\ddot{w}(x,t) = \frac{\partial^2 w}{\partial x^2}\dot{x}^2 + 2\frac{\partial^2 w}{\partial x \partial t}\dot{x} + \frac{\partial w}{\partial x}\ddot{x} + \frac{\partial^2 w}{\partial t^2}. \tag{23}$$

Substitution of the indicated derivatives from Eqs. (2) and (13) into Eq. (23) produces:

$$\ddot{w}(x,t) = (v_0 + a_0 t)^2 \underset{\sim}{G}_{xx}^T \underset{\sim}{D} + 2 (v_0 + a_0 t) \underset{\sim}{G}^T \underset{\sim}{\dot{D}} + a_0 \underset{\sim}{G}_x^T \underset{\sim}{D} + \underset{\sim}{G}^T \underset{\sim}{\ddot{D}}. \qquad (24)$$

The inertia force P^* associated with the moving mass, based upon Newton's second law, is:

$$P^* = -m \ddot{w}(x,t), \qquad (25)$$

where m is the mass of the moving load. To obtain equivalent nodal actions $\underset{\sim}{A}^*$ for the moving mass, Eqs. (24) and (25) are substituted into Eq. (5), which results in:

$$\underset{\sim}{A}^* = -\underset{\sim}{M}^* \underset{\sim}{\ddot{D}} - \underset{\sim}{C}^* \underset{\sim}{\dot{D}} - \underset{\sim}{S}^* \underset{\sim}{D}. \qquad (26)$$

The new identifiers in Eq. (26) are defined as follows:

$$\underset{\sim}{M}^* = m \underset{\sim}{G} \underset{\sim}{G}^T, \qquad (27)$$

$$\underset{\sim}{C}^* = m (v_0 + a_0 t) \underset{\sim}{G} \underset{\sim}{G}_x^T, \qquad (28)$$

$$\underset{\sim}{S}^* = m (v_0 + a_0 t)^2 \underset{\sim}{G} \underset{\sim}{G}_{xx}^T + m a_0 \underset{\sim}{G} \underset{\sim}{G}_x^T. \qquad (29)$$

It should be noted that the matrices $\underset{\sim}{M}^*$, $\underset{\sim}{C}^*$, and $\underset{\sim}{S}^*$ are all of order four, because they depend upon four shape functions of the loaded element. Inspection of Eqs. (27)–(29) reveals the fact that the matrix $\underset{\sim}{M}^*$ is symmetric while $\underset{\sim}{C}^*$ and $\underset{\sim}{S}^*$ are not. As a consequence, the coefficient matrices of the governing equations of motion for the system will also be unsymmetric, which complicates the solution technique somewhat.

The equivalent nodal actions associated with the moving mass are combined with those in Eq. (14) to give the equations of motion as:

$$\underset{\sim}{M} \underset{\sim}{\ddot{D}} + \underset{\sim}{S} \underset{\sim}{D} = \underset{\sim}{A} + \underset{\sim}{A}^*. \qquad (30)$$

Substitution of Eq. (26) into Eq. (30) and rearrangement of terms produces:

$$[\underset{\sim}{M} + \underset{\sim}{M}^*] \underset{\sim}{\ddot{D}} + \underset{\sim}{C}^* \underset{\sim}{\dot{D}} + [\underset{\sim}{S} + \underset{\sim}{S}^*] \underset{\sim}{D} = \underset{\sim}{A}. \qquad (31)$$

Eq. (31) shows that the mass and the stiffness matrices may be considered to be augmented by terms due to the moving mass. It is also of interest to note that the moving mass gives rise to terms associated with nodal velocities even when damping is not considered.

Numerical Integration

The linear acceleration method of numerical integration was utilized because it is well suited for second-order equations. The method is based upon the assumption that the nodal accelerations vary linearly during a small interval of time h and can be expressed (in matrix form) as:

$$\underset{\sim}{\ddot{D}}(t) = \underset{\sim}{\ddot{D}}_i + (\underset{\sim}{\ddot{D}}_{i+1} - \underset{\sim}{\ddot{D}}_i)\frac{t}{h}, \qquad t_i < t < t_{i+1}, \qquad (32)$$

where $\ddot{\underset{\sim}{D}}_i$ and $\ddot{\underset{\sim}{D}}_{i+1}$ are nodal accelerations at times t_i and t_{i+1}, respectively. Integration of Eq. (32) with respect to time yields expressions for velocities and displacements, which have the following values at the end of the interval:

$$\dot{\underset{\sim}{D}}_{i+1} = \dot{\underset{\sim}{D}}_i + \frac{h}{2}(\ddot{\underset{\sim}{D}}_{i+1} + \ddot{\underset{\sim}{D}}_i), \tag{33}$$

$$\underset{\sim}{D}_{i+1} = \underset{\sim}{D}_i + h\,\dot{\underset{\sim}{D}}_i + \frac{h^2}{6}(\ddot{\underset{\sim}{D}}_{i+1} + 2\,\ddot{\underset{\sim}{D}}_i). \tag{34}$$

Substitution of these expressions for time t_{i+1} into Eq. (31) produces a useful form for the equations of motion.

$$\left[\underset{\sim}{M} + \underset{\sim}{M}^* + \frac{h}{2}\underset{\sim}{C}^* + \frac{h^2}{6}\underset{\sim}{S} + \frac{h^2}{6}\underset{\sim}{S}^*\right] \ddot{\underset{\sim}{D}}_{i+1} =$$
$$\underset{\sim}{A}_{i+1} - \underset{\sim}{C}^*\left\{\dot{\underset{\sim}{D}}_i + \frac{h}{2}\ddot{\underset{\sim}{D}}_i\right\} - [\underset{\sim}{S} + \underset{\sim}{S}^*]\left\{\underset{\sim}{D}_i + h\,\dot{\underset{\sim}{D}}_i + \frac{h^2}{3}\ddot{\underset{\sim}{D}}_i\right\}. \tag{35}$$

Because all of the terms on the right-hand side of Eq. (35) are known at time t_{i+1}, it is possible to solve for the nodal accelerations $\ddot{\underset{\sim}{D}}_{i+1}$. Then the velocities and displacements may be evaluated by Eqs. (33) and (34).

Beam Example

The four-element beam model used for the moving-force problem was analyzed again for the moving-mass condition using the same physical constants. The ratio of the mass of the one-pound load to that of the beam is equal to 10.36 in this example.

Solutions for the moving-mass problem were obtained corresponding to the cases given previously for the moving-force problem. Fig. 7 shows plots of the dynamic response of the center of the beam for travel times equal to
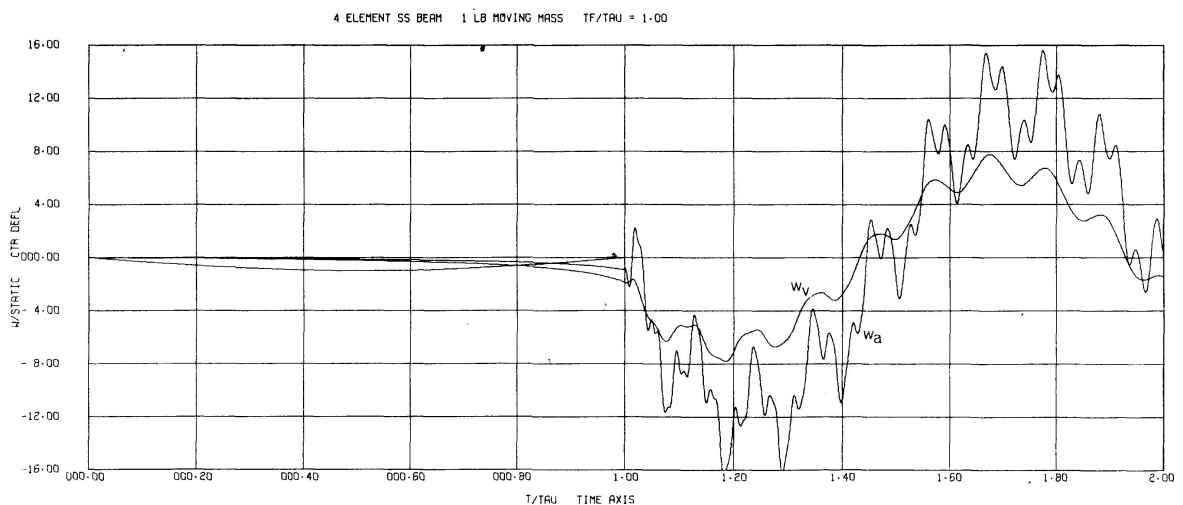

Fig. 7. Beam response to moving mass.

Table 3. Dynamic Magnification Factors for Moving Mass on Beam

$\dfrac{T_1}{T}$	$\dfrac{w_v}{w_{st}}$	$\dfrac{w_a}{w_{st}}$
(1)	(2)	(3)
$\frac{1}{8}$	1.216	1.331
$\frac{1}{4}$	2.783	4.000
$\frac{1}{2}$	5.507	12.93
1	7.748	15.72
2	6.105	10.61

the fundamental period. Dynamic magnification factors for the cases studied appear in Table 3, but no solutions were found in the literature with which to compare these results. Relative to the moving-force problem, however, the magnification factors are very large; and higher modes of vibration are excited, especially for the case of constant acceleration.

Plate Example

When one compares the linear dynamic responses of the beam and plate models subjected to moving forces, a great deal of similarity is seen to exist between the two sets of results (see Figs. 4 and 6). One would also expect results from the nonlinear analysis of the plate model traversed by a moving mass to be similar to those obtained for the beam. Because of this fact, and also due to the increased computer time required, plate solutions corresponding to the moving-mass beam solutions were not obtained. Instead, the effect of varying the mass ratio was studied for a series of constant-velocity runs.

The plate model used in the moving-force case was used again for the moving-mass case. After a few trial runs, attention was focused upon the constant-velocity ($v_0 = 1029\,\text{in./sec}$) corresponding to a travel time of $T_1/T = 0.25$. Numerical solutions for the dynamic response of the center of the plate
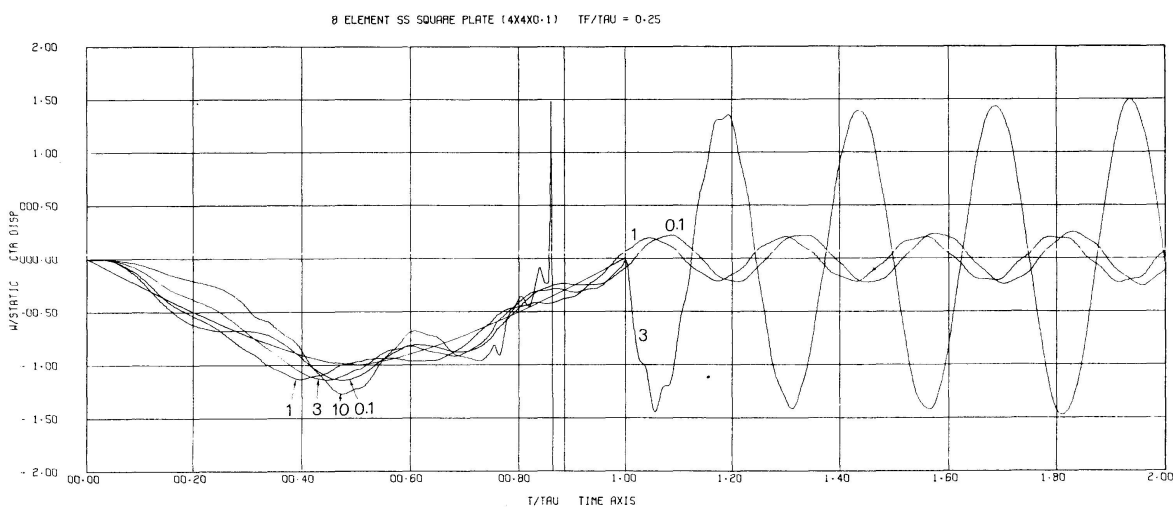

Fig. 8. Plate response to moving mass.

were obtained and are shown in Fig. 8 for four different mass ratios. Each curve in the figure is identified by its mass ratio (0.1, 1, 3, or 10).

It may be seen from the figure that the mass ratio has a dramatic effect upon the nature of the dynamic response. As the ratio is increased, the response of the plate becomes more pronounced until, for a mass ratio equal to 10, the center displacement becomes extremely large. The corresponding magnification factors for these four runs are: 1.125, 1.111, 1.505, and "extremely large".

Conclusions

As is true for numerous other applications, the finite-element method appears to be readily adaptable to problems of moving loads on structures. Computer programs with plotting capabilities are essential to the method. Documentation of the programs generated for this study may be found in Ref. [23] along with further details of the analytical methods and results.

Although the computer programs can accommodate various support conditions, only results for single-span beams and plates are reported herein. A radical change in the dynamic behavior of such structures occurs when the mass of the moving load is considered. The free-vibration response proved to be of greater interest than the forced response, and that for the accelerating mass was always larger than that for the constant-velocity case.

Feasible extensions to the present work include harmonic or random variation of the load, arbitrary path of travel on a plate, multiple loads, sprung masses, and damping. The assumption of constant acceleration of the load on a given element is not really a restriction because any time-history of velocity may be simulated by straight-line segments. Beams and plates on elastic foundations can also be modeled by the finite-element technique, as is explained in Ref. [23]. Inelastic and large-deflection analyses of beams and plates subjected to moving loads constitute additional areas of interest.

Notation

The following symbols are used in this paper:

$$\underset{\sim}{A} \;=\; \text{action vector}$$
$$\underset{\sim}{D} \;=\; \text{nodal displacement vector}$$
$$\underset{\sim}{G} \;=\; \text{shape function vector}$$
$$\underset{\sim}{M} \;=\; \text{mass matrix}$$
$$\underset{\sim}{S} \;=\; \text{stiffness matrix}$$
$$\underset{\sim}{r} \;=\; \text{column vector}$$
$$\underset{\sim}{x} \;=\; \text{normal coordinate}$$
$$\underset{\sim}{A} \;=\; \text{cross-sectional area of beam}$$

E = Young's modulus of elasticity
I = moment of inertia of beam
P = moving force
R = plate rigidity
T_1 = fundamental period
a_0 = acceleration coefficient
a,b = plate dimensions
h = time segment
l = length of beam element
m = moving mass
p = distributed force; natural frequency
t = plate thickness; time
x,y = space coordinates
v_0 = velocity coefficient
w = generic displacement
α = coefficient
λ = eigenvalue
μ = mass density
ν = Poisson's ratio
τ = dummy time variable
T = travel time

References

1. ARCHER, J. S.: "Consistent Mass Matrix for Distributed Mass Systems." Journal of the Structural Division, ASCE, Vol. 89, No. ST 4, Proc. Paper 3591, August 1963, pp. 161–178.
2. BIGGS, J. M., SUER, H. S., and LOUW, J. M.: "Vibrations of Simple-Span Highway Bridges." Trans., ASCE, Vol. 124, 1959, pp. 291–308.
3. BOGNER, F. K., FOX, R. L., and SCHMIT, L. A., JR.: "The Generation of Inter-Element-Compatible Stiffness and Mass Matrices by the Use of Interpolation Formulas." AFFDL-TR-66-80, Conference on Matrix Methods in Structural Mechanics, Wright-Patterson Air Force Base, Ohio, October 1965.
4. EICHMANN, E. S.: "Note on the Auxilary Effect of a Moving Force on a Simple Beam." Journal of Applied Mechanics, December 1953, p. 562.
5. FILHO, F. V.: "Dynamic Influence Lines of Beams and Frames." Journal of the Structural Division, ASCE, Vol. 92, No. ST 2, Proc. Paper 4797, April 1966, pp. 371 to 386.
6. FLEMING, J. F. and ROMUALDI, J. P.: "Dynamic Response of Highway Bridges." Journal of the Structural Division, ASCE, No. ST 7, Vol. 37, Proc. Paper 2955, October 1961, pp. 31–61.
7. HILLERBORG, ARNE: "A Study of Dynamic Influence of Moving Loads on Girders." Third Congress, Inter. Assoc. of Bridge and Structural Engineering, September 1948, pp. 661–667.
8. HILLERBORG, ARNE: "Dynamic Influence of Smoothly Running Loads on Simply-Supported Girders." Kungl. Tekniska, Hogskolan, Stockholm, 1951.

9. INGLIS, C. E.: "A Mathematical Treatise on Vibrations in Railway Bridges." Cambridge University Press, London, 1934.

10. JEFFCOTT, H. H.: "On the Vibration of Beams Under the Action of Moving Loads." Philosophical Magazine, Vol. 8, Series 7, 1929.

11. LANCZOS, C.: "An Iteration Method for the Solution of the Eigenvalue Problem of Linear Differential and Integral Operators." Journal Res. Nat. Bur. Stand., Vol. 45, 1950, pp. 255–282.

12. LOONEY, C. T.: "Impact on Railway Bridges." University of Illinois, Bulletin Series No. 352, 1944.

13. PRZEMIENIECKI, J. S.: Theory of Matrix Structural Analysis, McGraw-Hill, Inc., New York, 1968.

14. STOKES, G. G.: "Discussions of a Differential Equation Related to the Breaking of Railway Bridges." Trans. Cambridge Phil. Soc., Vol. 8, Part 5, 1867, pp. 707–735.

15. TIMOSHENKO, S. P.: "On the Transverse Vibrations of Bars of Uniform Cross-Section." Philosophical Magazine, Vol. 43, 1922, Paper 1018, pp. 125–131.

16. TUNG, T. P., GOODMAN, L. E., CHEN, T. Y., and NEWMARK, N. M.: "Highway Bridge Impact Problems." Bulletin 124, Highway Research Board, 1956, pp. 111–134.

17. VELETSOS, A. S., and HUANG, T.: "Analysis of Dynamic Response of Highway Bridges." Journal of the Engineering Mechanics Division, ASCE, Vol. 96, No. EM 5, Proc. Paper 7591, October 1970, pp. 593–620.

18. WEN, R. K.: "Dynamic Response of Beams Traversed by Two Axle Loads." Journal of the Engineering Mechanics Division, ASCE, Vol. 86, No. EM 5, Proc. Paper 2624, October 1960, pp. 91–111.

19. WILLIS, R.: "Report on the Commisioners Appointed to Inquire into the Application of Iron to Railway Structural Appendix." H. M. Stationery Office, London, 1849.

20. WILLIS, R.: "Treatise of the Strength of Timber, Cast Iron and Malleable Iron." London, 1851.

21. WILSON, E. L.: "A Computer Program for the Dynamic Stress Analysis of Underground Structures." SESM Report No. 68-1, University of California, Berkeley, California, January 1968.

22. WILSON, E. N. and TSIRK, A.: "Dynamic Behavior of Rectangular Plates and Cylindrical Shells." Civil Engineering Department Report No. S-67-7, New York University, October 1967.

23. YOSHIDA, D. M.: "Dynamic Response of Beams and Plates Due to Moving Loads." Ph. D. Thesis, Department of Civil Engineering, Stanford University, Stanford, California, May 1970.

Summary

The method of finite elements is used to model continuous beams and rectangular plates traversed by moving loads. Equations of motion for discretized beams and plates are solved for constant velocity and constant acceleration cases of moving loads with and without the influence of a mass associated with the load itself. Responde curves are compared with the results of other investigators wherever possible, but the methods utilized in this study are capable of producing results for problems not previously solved.

Résumé

La méthode des éléments finis est utilisée pour étudier le comportement en modèle réduit des poutres continues et des plaques rectangulaires sous l'influence de charges mobiles. Les équations de mouvement des poutres et plaques reproduites sont résolues pour les cas de vitesse et accélération constantes des charges mobiles, ceci avec ou sans l'influence d'une masse dépendante de la charge.

Les courbes d'oscillations sont, le cas échéant, toujours comparées à d'autres résultats; les méthodes utilisées dans ce travail donnent les résultats de problèmes jusqu'ici irrésolus.

Zusammenfassung

Die Methode der endlichen Elemente wird dazu verwendet, um durchlaufende Träger und rechteckige Platten bei bewegten Lasten modellmässig nachzubilden. Die Bewegungsgleichungen für diskretisierte Träger und Platten werden für die Fälle konstanter Geschwindigkeit und konstanter Beschleunigung bewegter Lasten mit und ohne Einfluss einer mit der Last selbst verbundenen Masse gelöst. Die Frequenzkurven werden, wenn immer möglich, mit den Ergebnissen anderer Forscher verglichen, aber die in dieser Arbeit verwendeten Methoden sind geeignet, Resultate von bisher nicht gelösten Problemen zu liefern.

Leere Seite

Blank page

Page vide